Available online at www.sciencedirect.com
SCIENCE DIRECT
Polymer 47 (2006) 2369–2380
polymer
www.elsevier.com/locate/polymer

The phase diagram of poly(4-hydroxybenzoic acid) and poly(2,6-hydroxynaphthoic acid) and their copolymers from X-ray diffraction and thermal analysis

Anton Habenschuss [a,*], Manika Varma-Nair [a,b,1], Yong Ku Kwon [a,b,2], Jisheng Ma [a,b], Bernhard Wunderlich [a,b]

[a] *Chemical Sciences Division, Oak Ridge National Laboratory, 1 Bethel Valley Rd., P.O. Box 2008, Mail Stop 6197, Oak Ridge, TN 37831-6197, USA*
[b] *Department of Chemistry, The University of Tennessee, Knoxville, TN 37996-1600, USA*

Received 22 December 2005; received in revised form 26 January 2006; accepted 27 January 2006
Available online 23 February 2006

Abstract

Homopolymers and copolymers of 4-hydroxybenzoic acid (HBA) and 2,6-hydroxynaphthoic acid (HNA) have been studied with differential scanning calorimetry and temperature-resolved wide angle X-ray diffraction. All polymers have more than one disordering transition between the glass transition (between 400 and 430 K) and decomposition (between 710 and 750 K). The first transition in PHBA at 616–633 K is from orthorhombic rigid crystals to a conformationally disordered pseudo-hexagonal phase (condis phase). The two higher transitions are first, a further disordering process to a hexagonal condis crystal, and then a change to an anisotropic melt (liquid crystal) at about 800 K, with increasing decomposition above 750 K. In PHNA, orthorhombic crystals change above 600 K to an orthorhombic condis crystal structure, which go to an anisotropic melt at 750 K, and subsequent decomposition. In addition, using empirical entropy rules that account for the changes during the transitions from the crystal to the disordered mobile phases, an effort is made to understand the disorder and mobility, and to arrive at a non-equilibrium phase diagram of the copolymer system. The existence of a single, but up to 200 K wide, glass transition and remaining high crystallinity of the copolyesters, indicate partial solubility of the repeating units in all phases. The new data are compared to and brought into agreement with the large number of prior measurements and often unclear interpretations.

Keywords: Poly(4-hydroxybenzoic acid); Phase diagram; Poly(2,6-hydroxynaphthoic acid)

1. Introduction

In the past, the structures and transitions of main-chain liquid crystalline polymers have been extensively studied. The three-dimensional structures of poly(4-hydroxybenzoic acid) (PHBA) and poly(2,6-hydroxynaphthoic acid) (PHNA) have been of particular interest, owing to their physical properties and industrial applications [1–4]. Copolymers of 4-hydroxybenzoic acid (HBA) and 2,6-hydroxynaphthoic acid (HNA) have also been produced with the aim of improving moldability and processability [5]. The chemical structures of PHBA and PHNA are shown below.

PHBA PHNA

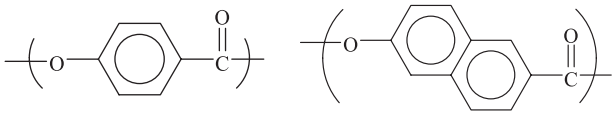

(1)

The earlier studies of both homopolymers have shown two or more phase transitions before isotropization or thermal decomposition [6–14]. For PHBA, the lower transition is identified as a crystal (orthorhombic, polymorphs I and II) to a conformationally disordered crystal (pseudo-hexagonal) transition [11,12]. Conformationally disordered (condis) crystals show large-amplitude, internal-rotational mobility [15]. Based on its molecular structure, it has also been called a one-dimensional plastic crystal or an ordered smectic phase. On cooling, a condis crystal freezes into a solid condis glass [15], a most important transition because it limits most of its applications. The next transition in PHBA involves an additional disordering process. A

* Corresponding author. Tel.: +1 865 574 6018; fax: +1 865 576 7956.
E-mail address: habenschussa@ornl.gov (A. Habenschuss).
[1] Present Address. Exxon Mobil Research and Engineering Co., NJ, USA.
[2] Present Address. INHA University Nam-Ku, Inchon, South Korea.

0032-3861/$ - see front matter © 2006 Elsevier Ltd. All rights reserved.
doi:10.1016/j.polymer.2006.01.088

small, broad endotherm with an entropy of transition of about 0.4 J K^{-1} mol^{-1} has been observed at around 715 K and is shown to involve no change in the packing-order along the chain axis or chain conformation, but a loss of long range phenyl orientation in the *a–b* plane. An indication of the ultimate melting of whiskers and slabs (single crystals) of PHBA and PHNA was also reported above 800 K, based on DSC at 20 K min^{-1} [14,16], but these transitions are accompanied by considerable decomposition.

Much less information is available about the structure of PHNA. Prior calorimetry in our laboratory has shown a broad transition at about 614 K [8,9]. Existence of a second, sharp, large transition at 726 K with an entropy of transition of 6.0 J K^{-1} mol^{-1} became evident from the work of Mühlebach et al., using differential scanning calorimetry (DSC), thermo-mechanical analysis (TMA) and electron and optical microscopy by extending the measurements into the decomposition region [13]. This second transition leads to a more mobile mesophase that has been proposed to be a nematic liquid crystal. In addition to DSC, infrared spectroscopy (IR), optical microscopy and X-ray studies were carried out on whiskers of PHNA beyond the second transition [14]. A large endotherm above 800 K is in the decomposition region. The transition at about 610 K involves a change from orthorhombic to nearly pseudo-hexagonal, which changes at about 720 K to a phase in which the naphthalene units possess considerable rotational freedom [14].

The thermal properties of the copolymers, which are statistical in nature, have been studied in considerable detail up to 650 K (somewhat below decomposition), including heat capacity, C_p, enthalpy, entropy and Gibbs function, and the transition behavior [8,9]. The reversibility of some of the transitions has been analyzed by temperature-modulated DSC and is to be reported in a later publication [17]. The glass transitions of the copolymers are located at 405–430 K and are rather broad (160–200 K wide). Their ΔC_p changes little with composition (35–42 J K^{-1} mol^{-1}) [9]. The C_p for the crystal, glass, and anisotropic melt is additive relative to the homopolymers, which is lost in the glass-transition region. The low-temperature disordering of the copolymers appeared to define a eutectic-like phase diagram [8,13]. A revised interpretation and a first complete phase diagram which include the higher transitions are presented in this paper. Crystallization of the 75, 58, and 30 mol% HBA copolymers shows a fast process to a pseudo-hexagonal phase, and a slow process to orthorhombic crystals [7]. The kinetics was reported based on calorimetry [10] and X-ray analysis [18].

The X-ray diffraction data of the copolymers reveal a high-axial orientation and three-dimensional order while the meridional reflections are aperiodic. The molecular structure of the copolyesters is rather interesting. Biswas and Blackwell [19–21] proposed that the structure of the copolymer with a 75/25 composition of HBA/HNA consists of arrays of parallel chains of the random copolymer sequence in a para-crystalline structure [5]. In their model, the definition of chain register is where one monomer on each chain is in the same horizontal plane. The repeat distance along the fiber axis is equal to the average dimer length. A different model of non-periodic layers was proposed by Windle and coworkers [22–24]. In this model, the matching is calculated for short sequences of identical chemical structure from their random occurrence in parallel chains. Such a model was earlier used for a computer evaluation of accidental matches on cold crystallization of copolymers of poly(ethylene terephthalate-*co*-sebacate) [25]. A more detailed comparison of the two models is given in [26]. The structure above the disordering transition was suggested to be a condis crystal with rotational disorder, this is also supported by evidence from mechanical and dielectric relaxation measurements [12,27,28].

Initial phase diagrams and the transitions in the HBA and HNA copolymer system have been the subject of several studies [8,9,13]. The general features of the phase diagram and the number of transition in the HBA/HNA copolymers is by now fairly well established, but the nature of some of the phases is still a matter of some controversy. Some of these uncertainties stem from the metastable nature of the phases and the slow kinetics involving physical as well as chemical equilibria. These polymers are easily crystallized either on cooling or quenching, and their thermal history must be considered prior to measurement. In this study, we carried out X-ray analyses to resolve the nature of the high-temperature transitions in PHBA and PHNA and extended the work to the copolymers. Overall, we arrive at an improved phase diagram which is in accord with much of the large literature on the subject.

2. Experimental

2.1. Materials

The polymers used in this study were composed of HBA and HNA with mole ratios of 100/0, 95/5, 90/10, 80/20, 75/25, 58/42, 30/70 and 0/100 (the HBA component is listed first), which were commercial samples, prepared as described in [29], provided by Hoechst–Celanese Research Co. in the form of pellets (H–C, commercial samples). These as-received, pelletized samples were used without further treatment. In addition, some single crystals of PHBA and PHNA were kindly provided by Prof. H.R. Kricheldorf of the University of Hamburg (K, K–A, and K–B samples). Preparation and characterization of these samples are described in [30,31] and [14], respectively.

2.2. Wide angle X-ray diffraction

The X-ray experiments were performed on a Scintag PAD-X X-ray powder diffractometer in reflection geometry, using unfiltered Cu K_α radiation ($\lambda = 1.5418$ Å) (except for the 80/20 copolymer, where Mo K_α radiation was used, instead). Energy discrimination of the scattered radiation was accomplished with a Peltier-cooled solid-state detector. The bulk-molded polymer pellets were ground to a fine powder in liquid nitrogen to produce an averaged crystal arrangement. The K samples were in the form of fine whiskers, and were used as such

without further preparation. The powder samples, aggregated to an overall dimension of $10\times7\times1$ mm^3, were placed on a resistively heated tantalum strip which served as the sample stage. The temperature of the sample was controlled by passing a current directly through the strip, and the temperature controller provided an accuracy of about ±2 K.

X-ray data were collected in the 2θ range 6–56° using a 0.1° step size. Typically, two series of temperature scans were made for each sample. First, quick scans were made in order to estimate the approximate temperatures of the structural transitions. Then a series of longer scans as a function of temperature were made to achieve diffraction patterns of good precision. The peak positions were determined by deconvolution using pseudo-Voigt functions, and the unit cell parameters were refined by the program developed by Appleman [32].

2.3. Differential scanning calorimetry

Thermal analysis was performed on a Perkin–Elmer DSC 7 thermal analyzer, equipped with a dry box assembly, necessary to avoid signal instability due to drafts or changes in room temperature. Low-pressure dry nitrogen gas was kept flowing at constant rate through the dry box to prevent condensation from the atmosphere. During measurements, dry nitrogen gas was allowed to flow through the DSC cell at a rate of 20 mL min^{-1}. The temperature signal was calibrated by the onset of melting of indium and cyclohexanone at a heating rate of 10 K min^{-1}, and the heat flow rate was calibrated by the heat of fusion of indium.

The glass-transition temperatures, T_g, were taken, as usual, at the temperature of half-devitrification of the sample at the given heating rate. The samples were cooled before analysis at a similar rate to minimize enthalpy relaxation (hysteresis). The width, ΔT, of the glass transition region was estimated from the intersection of a tangent to the point of inflection, which is close to T_g, with the baselines of the glass and melt heat capacities. For amorphous homopolymers and random copolymers, this width of ΔT should be between 5 and 10 K, for the partially ordered HBA/HNA copolymers, this range increases to as much as 200 K [8,9]. The first-order transitions are approximated by the peak temperatures, representing melting of the most common species.

3. Results

3.1. Differential scanning calorimetry

Fig. 1 shows typical DSC scans of the as-received homopolymers PHBA and PHNA and three of the copolyesters measured with a heating rate of 20 K min^{-1}. Thermogravimetric studies under nitrogen showed that the two homopolymers and the copolyesters with higher HBA contents (95, 90 and 80 mol%) heated at the same rate begin thermal decomposition prior to their isotropization [9], the DSC measurements were, therefore, limited to 750 K. The upper left curves of Fig. 1 show the DSC data of the PHBA homopolymer. In the top scan, for example, two endothermic peaks were detected one at 633 K with an estimated ΔS of

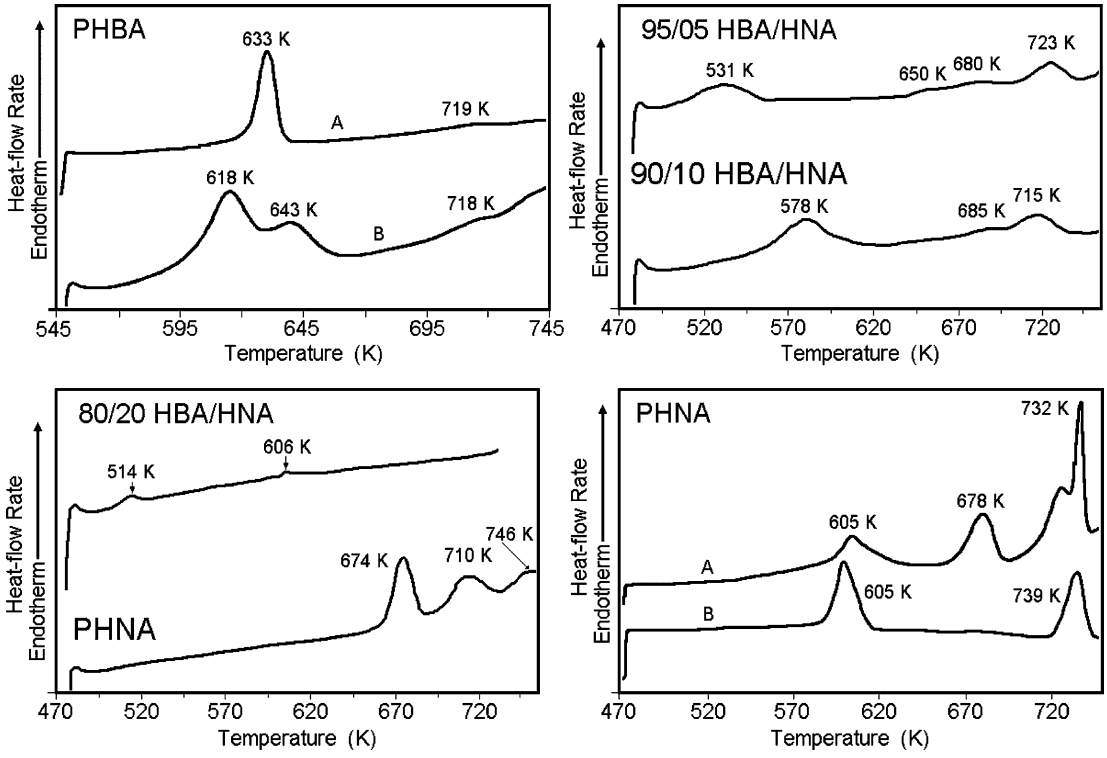

Fig. 1. Typical DSC scans of as-received homopolymers PHBA and PHNA and some of their copolyesters, using a heating rate of 20 K min^{-1}. Upper left: PHBA, single-crystal whiskers (A) and commercial sample (B). Upper right: copolymer 95/5 and 90/10. Lower left: copolymer 80/20 and PHNA commercial sample. Lower right: PHNA single crystal whiskers of type K–A and K–B.

Table 1
Thermodynamic parameters for the disordering transitions

HBA/HNA	T_g[a] (K)	T_1 (K)	ΔS_1 (J K^{-1} mol^{-1})	T_2 (K)	ΔS_2 (J K^{-1} mol^{-1})	T_3 (K)	ΔS_3 (J K^{-1} mol^{-1})
100/0[b]	–	633	9.3	719	0.5	–	–
100/0[c]	434	618+643	8.7	718	0.1	–	–
100/0[d]	–	621	8.4	711	0.4	–	–
95/5	430	531	1.5	650+680	0.06+0.12	723	0.5
90/10	427	578	3.1	685	0.05	715	1.7
80/20	425	514	0.2	–	–	606	0.9
75/25[e]	405	547	0.9	–	–	565	0.2
58/42	415	511	0.5	–	–	523	0.4
30/70[e]	418	579	0.5	–	–	579	?
0/100 [f]	–	605+678	2.8+2.2	–	–	732	3.8
0/100 [f]	–	605	10.0	–	–	739	6.5
0/100[c]	420	674+710	3.2+1.6	–	–	746	~0.6
0/100[d]		611	8.5	–	–	726	6.0

The molar mass of the HBA and HNA repeating units are 120.1 and 170.2 Da, respectively. The entropy changes are estimates from the measured enthalpy of transition divided by the peak temperature as listed in the table, i.e. they are estimates, not equilibrium entropies.

[a] The glass transition temperatures, T_g, were determined on the same samples together with a heat capacity analysis in [9]. The increase in heat capacity at T_g was, as expected, 34–45 J K^{-1} mol^{-1}.

[b] Data on single crystal whiskers prepared by Kricheldorf [29,30].

[c] Commercial samples H–C. As-received PHBA and PHNA samples have double peaks, as listed. In PHNA, annealing at 590 K lowers the first peak temperature while increasing the second.

[d] Data from [12].

[e] The data for the metastable disordering for the annealed orthorhombic phase from [9] are: for the 75/25 copolymer $T_d^0 = 610$ K and $\Delta S_d^0 = 6$ J K^{-1} mol^{-1} and for the 30/70 copolymer, 630 K and 7.4 J K^{-1} mol^{-1}, respectively.

[f] Data on crystal whiskers prepared by Kricheldorf, samples A and B of [14]. The here presented values of T_1 and T_3 are close to the reported temperatures in [14] when omitting the higher endotherms.

9.3 J K^{-1} mol^{-1} and one at 719 K with $\Delta S = 0.5$ J K^{-1} mol^{-1}. The entropy changes were estimates from the measured enthalpy of transition, divided by the peak temperature. Note, that neither is the peak at the equilibrium temperature, nor does the heat of transition represent pure phases because of the semi-ordered nature of the polymers. The first endotherm represents the formation of a condis crystal from the rigid crystal, and the second endotherm is very small. The data for all homopolymers and copolymers are collected in Table 1. The commercial sample showed double endothermic peaks in the temperature range of 595–670 K. These multiple endotherms appear to be due to different thermal histories of the skin and core of the pelletized polymer. The existence of multiple melting of lesser separation of not as perfect whisker-like crystals of PHBA which were prepared at low temperature and short reaction time was also reported [30]. The DSC scans of PHNA illustrate the breadth of the melting behavior for samples of different history. Again, the lower endotherms are due to a change from a rigid crystal to a condis crystal, whereas a significant amount of entropy of transition is also associated with the higher endotherms indicating that significant further mobility is initiated at the higher temperatures.

In the upper right DSC scan of Fig. 1 the as-received 95/5 copolymer shows a series of rather small endothermic peaks in the temperature range of 500–750 K. The first endotherms at 531 and 650+680 K were assigned to rigid-to-condis crystal and condis-to-condis crystal transitions, similar to those observed in the PHBA homopolymer. In addition, the highest endotherm found at 723 K leads to a change of the condis crystal to an anisotropic melt. A similar DSC result was also found for 90/10 copolyester.

For the 80/20 copolymer in the lower left DSC traces of Fig. 1, due to the imperfection of the crystal structure, the two endothermic peaks were found at 514 and 606 K, lower than those from 90/10 copolymer. The intermediate condis-to-condis transition is missing. The entropies associated with both transitions were also smaller than those from the copolymers, 95/5 and 90/10. As the HNA content increases from 25 to 70 mol%, the two small endotherms approach each other, indicating little or no intermediate condis phase. The substantial crystallinities found by X-ray diffraction within the copolymers of this large HNA content are probably due to an isomorphism of the HBA and HNA monomers, as proposed by Biswas and Blackwell [19–21] or the accidental match of parallel repeating units as proposed by Windle and Coworkers [22–24]. The quantitative information on the copolymers, as well as the details of the samples of the different PHNA samples beyond the above summary are given in Table 1 and its footnotes.

3.2. X-ray diffraction

To verify the various phases in the homopolymers and establish the nature of the phases for the copolymers with 5, 10 and 20 mol% HNA, temperature-resolved wide angle X-ray diffraction patterns were generated and analyzed. Typically, a set of quick scans (minutes) were taken to

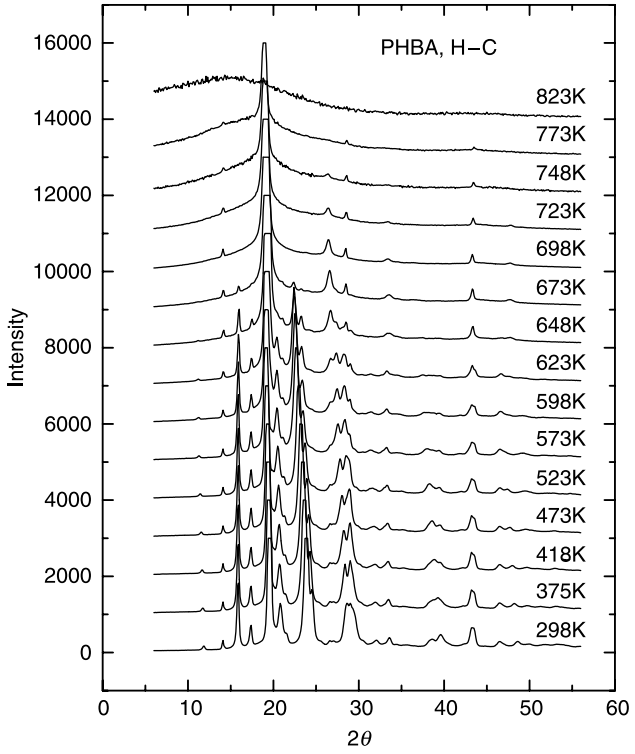

Fig. 2. X-ray diffraction scans of commercial sample PHBA (H–C) as function of temperature.

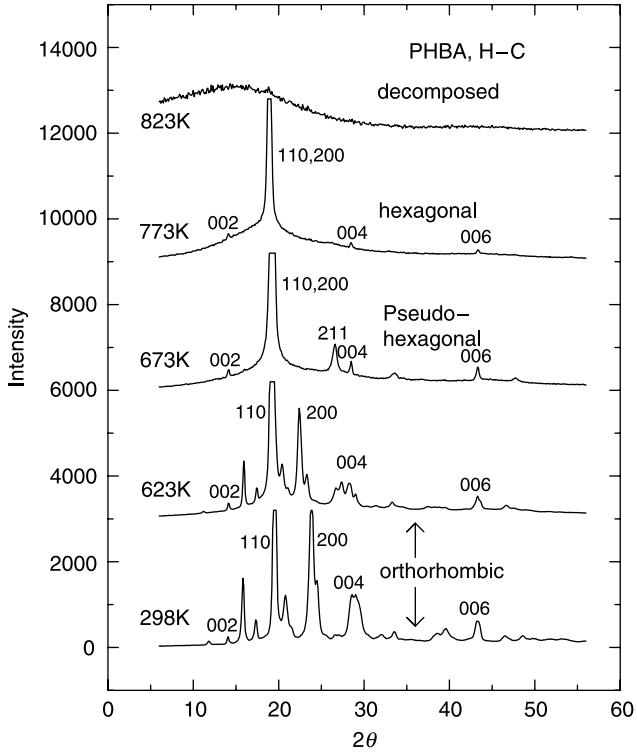

Fig. 3. X-ray diffraction patterns of the various PHBA (H–C) phases.

identify the transition temperatures. Longer scans (~hours) were then taken at each temperature to obtain good diffraction patterns. No obvious differences in the diffraction patterns between the short and longer scans were observed. Except near decomposition, samples were not sensitive to long-term exposure of either high temperature or to radiation. The resulting diffraction patterns and their analysis are presented in Figs. 2–11.

3.2.1. PHBA

Fig. 2 shows a series of the X-ray diffractometer scans of the commercial H–C sample of PHBA, recorded as a function of temperature from room temperature to decomposition at 823 K. The PHBA is highly crystalline with a relatively sharp diffraction pattern for a polymer. The structure of PHBA at room temperature was shown to contain the two crystalline modifications with orthorhombic unit cells [33–35]. Iannelli and Yoon [36] refined the crystal structure of PHBA by using a Rietveld analysis and proposed that the molecular structure of PHBA is a mixture of the two orthorhombic phases with the following parameters: $a=7.42$ Å, $b=5.70$ Å, and $c=12.45$ Å for phase I; and $a=3.83$ Å, $b=11.16$ Å, and $c=12.56$ Å for phase II. Assuming a bimorphic behavior of the orthorhombic crystalline phase of PHBA, we derived the unit cell parameters for our observed diffraction peaks recorded at room temperature based on the program developed by Appleman [32]. A reasonable match between the observed and calculated data could be reached with parameters $a=7.46$ Å, $b=5.72$ Å, $c=12.72$ Å, $V=543$ Å^3 for phase I; and $a=3.87$ Å, $b=11.20$ Å, $c=12.59$ Å, and $V=546$ Å^3 for phase II.

Changes in the X-ray diffraction patterns in Fig. 2 can be seen near 650 and 750 K, which are consistent with the DSC results on PHBA in Table 1, where two endothermic peaks are listed for the same sample at 620–640 and 718 K. Many of the diffraction peaks disappear above 623 K. Above 718 K, a single major diffraction peak dominates the scan. In Fig. 3 we show typical diffraction patterns within the temperature regions of constant structure. The lowest two curves are of the orthorhombic phases and show a shift in the 110 peak and an even larger shift in the 200 peak in going from room temperature to just before the first transition at 650 K. On the other hand, the 00l-peaks (002, 004, and 006) remain almost constant over this region.

In the temperature range of 650–750 K, a more symmetric structure appears. The phase in this temperature region, exemplified by the 673 K pattern in Fig. 3, shows an intense peak at $2\theta\approx18.9°$, indicating a hexagonal unit cell. However, the 211 reflection at $2\theta\approx26.5°$ should be absent in a truly hexagonal structure, and indicates that the structure is only metrically hexagonal, i.e. is a so-called pseudo-hexagonal phase. Formally, therefore, the transition to this phase is an orthorhombic–orthorhombic transition. In addition, the 00l reflections remain evident.

On further heating to 773 K, the 211 reflection disappears, and the structure transforms to a true hexagonal phase. The weak, but sharp, 002, 004 and 006 reflections remain, indicating that this remains a true (condis) crystalline phase, and is not an anisotropic melt or liquid crystal.

On heating to 823 K, only a broad diffraction halo remains in Figs. 2 and 3. Cooling to room temperature at this stage indicates that the sample had undergone thermal decomposition,

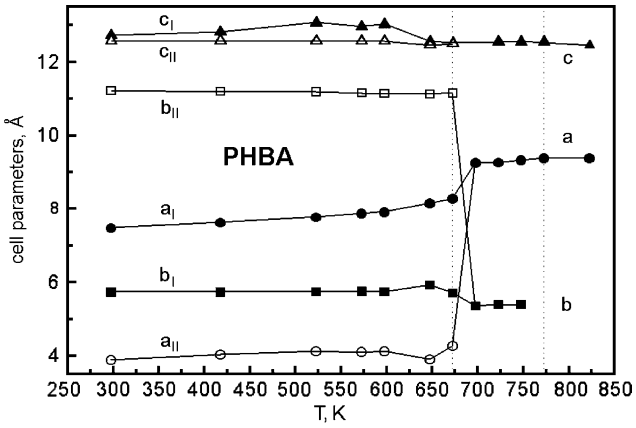

Fig. 4. PHBA unit cell parameters of orthorhombic polymorphs I and II as a functions of temperature.

as opposed to melting. This decomposition was previously documented by thermogravimetry on the same samples [9]. In contrast, cooling from the hexagonal phase at 773 K to room temperature, the orthorhombic structure is recovered.

Fig. 4 shows unit cell parameters of the PHBA in the temperature range of 300–825 K. The a dimensions of both orthorhombic I and II phases expand up to 650 K, while the b and c dimensions remain almost constant (the chain axis is in the c-direction). At 650 K the a and b parameters change abruptly to values close to a ratio of $3^{1/2}$, indicating the transformation of the orthorhombic crystals into the pseudo-hexagonal symmetry. At this temperature the volume of the unit cell increases by approximately 12%, which originates mostly from the increase in the cross-sectional area per chain. The phase transition from the pseudo-hexagonal to hexagonal unit cell at 750 K is not accompanied by any abrupt changes in the unit cell in agreement with the very small entropy estimate.

3.2.2. PHNA

Fig. 5 shows a series of typical diffraction data on the as-received H–C PHNA, recorded during heating. The diffraction patterns of PHNA show fewer and broader peaks than were found for PHBA. Over the temperature range from 293 to 823 K, the X-ray data showed clear changes near 600 and 740 K, which are consistent with the broad range of DSC results of Table 1. Fig. 6 shows the structure assignment. At 293 K we find an orthorhombic structure which was indexed with unit cell parameters of $a=7.80$ Å, $b=5.90$ Å, $c=16.85$ Å and $V=775$ Å^3. On heating, this orthorhombic structure persists up to 523 K, with the 200 peak moving to lower 2θ values. At the first transition, around 600 K in Fig. 6, the 200 reflection at 23° disappears, and a new reflection grows-in at $\approx 19°$ as a shoulder on the intense 110 peak. This shoulder could be identified with the 200 reflection of a new orthorhombic unit cell. Unlike in PHBA, the structure does not convert to a pseudo-hexagonal structure, but becomes a new orthorhombic structure, which is 'almost' pseudo-hexagonal. Note that the 211 reflection of this new orthorhombic structure is present. Thus this is also an orthorhombic–orthorhombic transition.

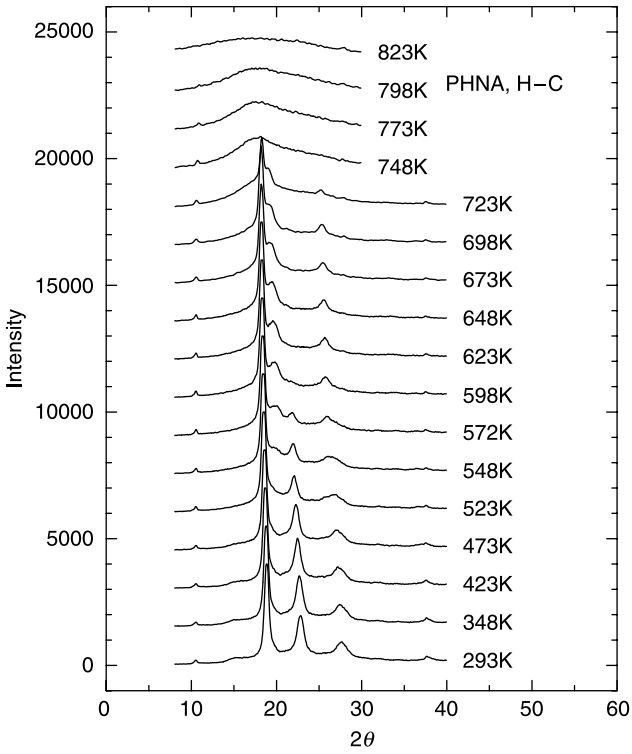

Fig. 5. X-ray diffraction scans of commercial sample PHNA (H–C) as function of temperature.

The second transition occurs near 740 K, where the peaks from the second orthorhombic structure disappear except for the small, but sharp 002 reflection. The 110 and 200 never merge as in PHBA and the 211 is also present until it

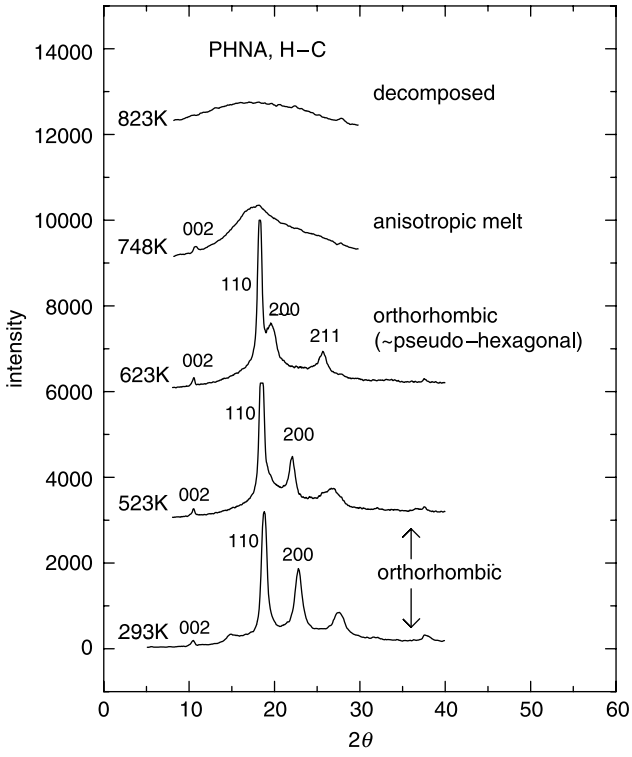

Fig. 6. X-ray diffraction patterns of the various PHNA (H–C) phases.

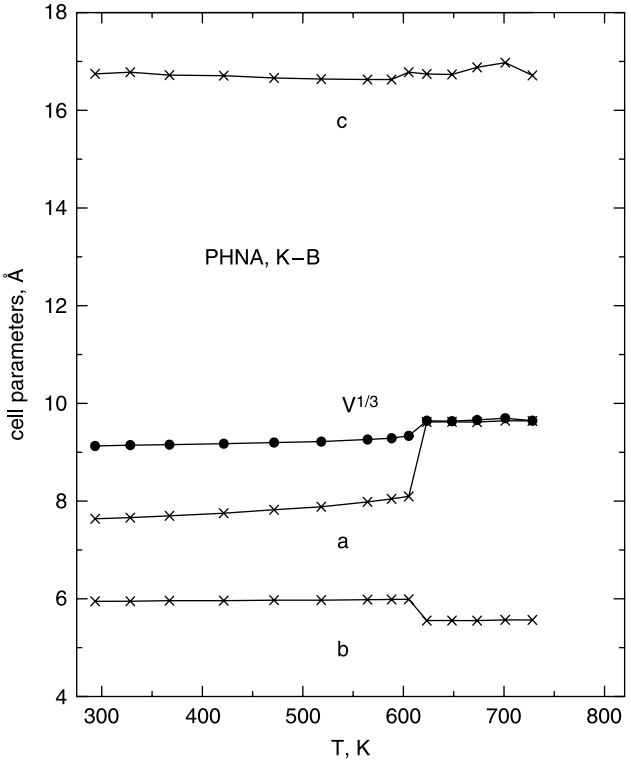

Fig. 7. Unit cell parameters of PHNA (K–B) as a functions of temperature.

disappears together with the 110 and 200. Thus the second orthorhombic structure transform into the new phase without ever becoming pseudo-hexagonal or hexagonal as in PHBA. The diffraction pattern of this new phase above 740 K is amorphous-like, except for the weak, but sharp 002 reflection. This phase is, therefore, an 'anisotropic melt'. Long-range lateral correlations in the *a–b* plane are lost, but long-range correlations along the *c*-direction remain, indicated by the 002 reflection. Lowering the temperature from 773 K recovers the second orthorhombic phase, verifying the high-temperature phase is not a decomposition product, but a mobile phase. The magnitude of the DSC endotherm at 746 K corresponding to this phase transformation is consistent with a loss of positional order in two-dimensions. Previous polarized optical microscopy study [13] also confirmed the anisotropy of the melt at this temperature which is typical of a liquid-crystal-like texture. On further heating, major thermal decomposition has occurred near 800 K.

The K–B sample shows essentially the same behavior; although the unit cell parameters at room temperature are slightly different: $a=7.64$ Å, $b=5.95$ Å, $c=16.71$ Å, $V=760$ Å^3. Also, the 00l reflections are weak to absent in this sample, which may have suffered from preferred orientation due to the anisotropic habit of the sample whiskers. The unit cell parameters of the K–B PHNA are shown in Fig. 7. The cell parameters behave very similarly to those of PHBA, with *a* slowly increasing up to the first transition at 600 K, while *b* and *c* remain almost constant. The volume increase at the 600 K transition is about 10%.

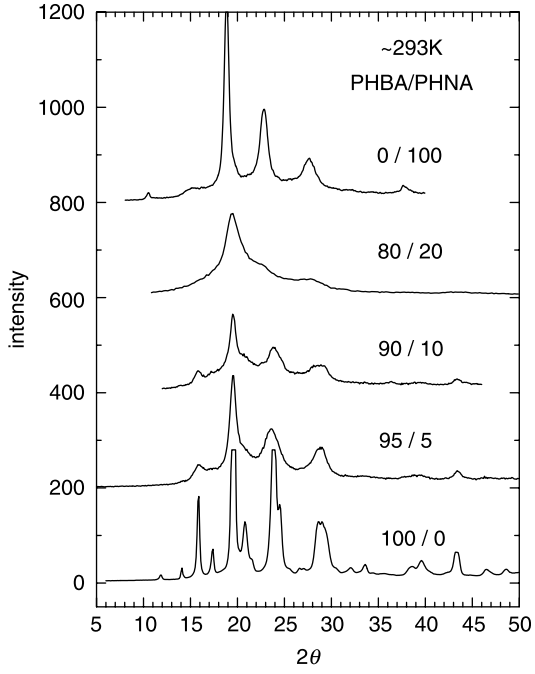

Fig. 8. X-ray diffraction patterns of PHBA/PHNA copolymers at 293 K.

3.2.3. The HBA/HNA copolymers

Fig. 8 shows the diffraction patterns of the HBA/HNA copolymers at room temperature. It is clear that the 100% PHBA shows the most structure and crystal perfection, while the 100% PHNA has fewer and broader diffraction peaks than those in PHBA. As more HNA monomer is introduced in the 95/5, 90/10 and 80/20 copolymers, the number of diffraction peaks decreases, and they become broadened. However, in all cases the main three peaks remain, which correspond to the orthorhombic structure at room temperature.

In Fig. 9 the diffraction patterns of the H–C 95/5 copolymer are presented. In these data, the diffraction peaks were fewer and broader than for the PHBA homopolymer, which may be due to the crystal imperfection of the 95/5 copolymer generated from the addition of the HNA comonomer. Four structures can be identified: the orthorhombic structure at room temperature, a pseudo-hexagonal phase at 573 K, a true hexagonal phase at 696 K, and an anisotropic melt at 773 K. At 808 K the 95/5 copolymer decomposes thermally. These phases parallel those of the 100% PHBA, except for the anisotropic melt in 95/5. In general, the diffraction patterns are markedly broadened, and many fewer peaks are present compared to the pure PHBA of Fig. 3. The addition of 5 mol% HNA comonomer decreases structural regularity and order of the PHBA chains. The 00l reflections are weak and not well defined at higher temperatures. Therefore, evidence for long-range correlation in the *c*-directions is not discernable for the anisotropic melt.

Fig. 10 shows the diffraction patterns of the 90/10 copolymer. Compared to the 95/5 copolymer, the peaks in the 90/10 copolymer are even broader and weaker. Nevertheless, the same four phases are present in this copolymer: orthorhombic at 293 K, pseudo-hexagonal at 648 K, true hexagonal at 698 K, an anisotropic melt at 748 K, and thermal decomposition at 793 K.

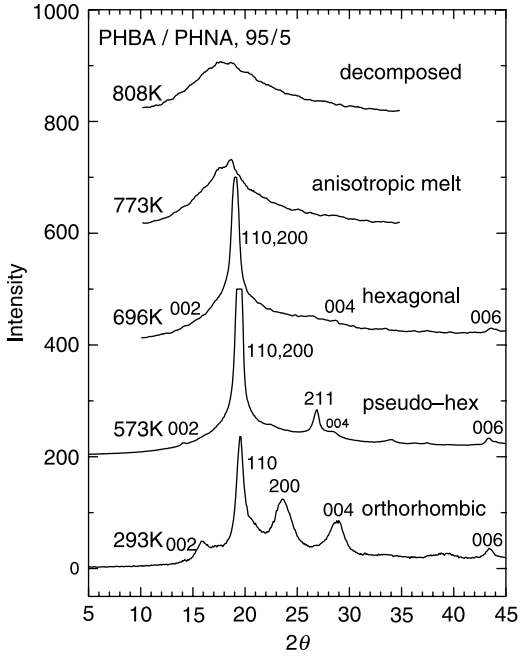

Fig. 9. X-ray diffraction patterns of 95/5 PHBA/PHNA copolymer.

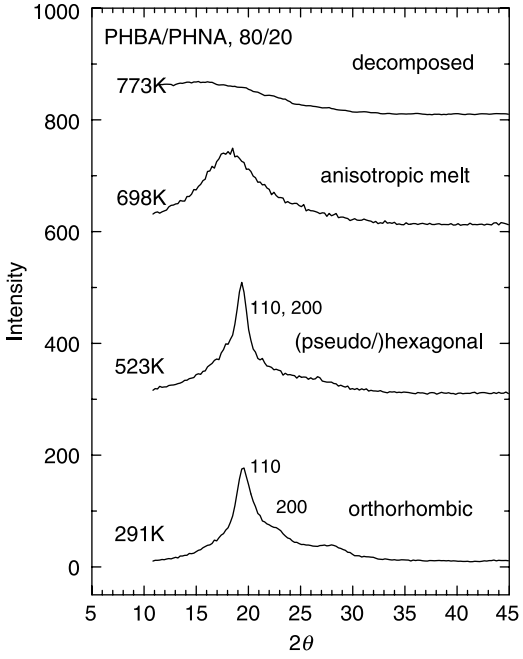

Fig. 11. X-ray diffraction patterns of 80/20 PHBA/PHNA copolymer.

All the transition temperatures are lower than in the 95/5 copolymer. The peaks at $2\theta = 22.5$, 28, and 36.5°, most evident in the anisotropic melt and the decomposed material, are tantalum reflections stemming from the sample stage heater.

Fig. 11 shows the X-ray diffractometer scans of the as-received 80/20 copolymer. For the 80/20 copolymer, the disordering in the chain direction due to the incommensurate length of the respective monomer repeating units is so great that all the features of the diffraction patterns are extremely broadened. Yet, the transition from the orthorhombic phase to the condis phase is still discernible, in that the three peaks of the former are replaced by the single reflection in the condis phase. However, the pseudo-hexagonal-to-hexagonal transition is no longer resolved in the 80/20 copolymer. The anisotropic melt at 698 K is still present. The increasing amount of the HNA comonomer in the copolymers increases the structural disorder, and the chain mobility of the rigid PHBA chains leads to more rotational freedom.

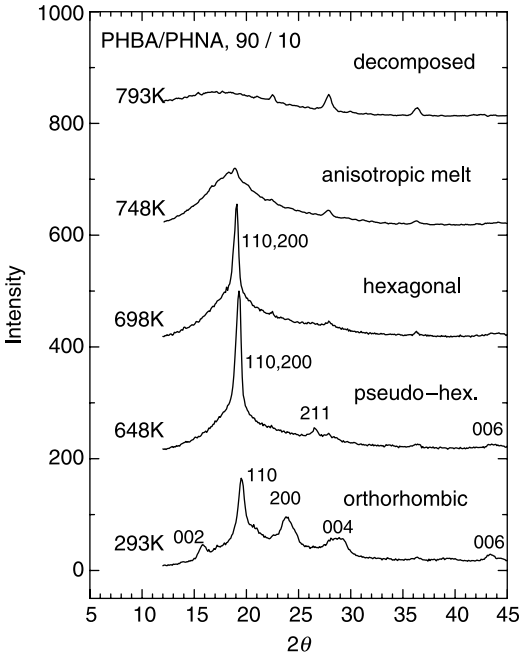

Fig. 10. X-ray diffraction patterns of 90/10 PHBA/PHNA copolymer.

3.3. A phase diagram

A combination the calorimetric information of Table 1 and the X-ray data of Figs. 2–11 is displayed in Fig. 12 in form of

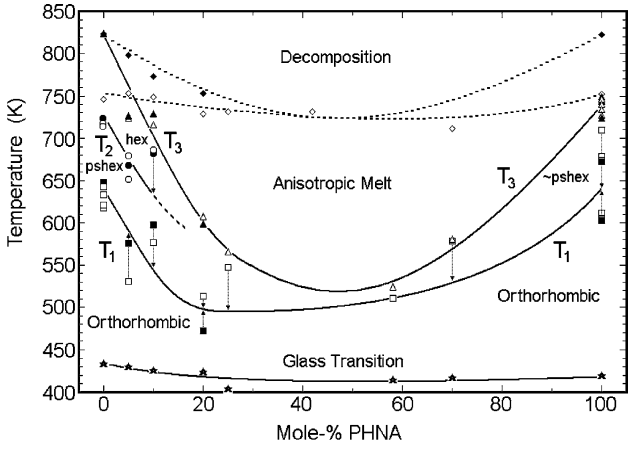

Fig. 12. Phase diagram of the copolymer system HBA/HNA without annealing. Filled symbols are based on X-ray data, open symbols, on thermal analysis. The decomposition temperatures (◇) represent 20% loss of mass of the commercial samples (at a heating rate of 20 K min^{-1} under nitrogen) [9]. The glass transition temperatures (★) are based on the heat capacities of the commercial samples [9].

a phase diagram. The rather large variation of the data points can be linked to the changing physical and chemical histories of the samples, i.e. the phase diagram represents a non-equilibrium diagram, approximating the samples analyzed. At high temperature, decomposition limits the diagram. At lower temperature, the nature of the phases is changed by the appearance of the glass transition. One must remember that the HBA/HNA copolymer system is characterized by exceedingly broad glass transitions. The glass transition region reaches easily up to the first disordering transition T_1. Since the increase in heat capacity is as expected for a conformationally fully excited molecule of a repeating unit of two parts (1 small + 1 large bead), it is likely that disordered phase as well as crystal participate in the glass transition [37].

4. Discussion

4.1. Homopolymer and copolymer crystals and glasses

The special property of PHBA is the sharp X-ray diffraction diagrams seen in Figs. 2 and 3 in the commercial and, even more-so, in the single-crystal samples. The orthorhombic crystal structures I and II of [36] could be fitted to the present data, as shown in Figs. 3 and 4. Early electron micrographs and diffraction patterns revealed lamellar platelets with a single crystal structure [33–35]. Detailed analyses of single crystals in form of whiskers and platelets [30,38,39], and thin lamellae [40–42] confirmed the high degree of regularity possible in PHBA and the two orthorhombic crystal structures. The method of crystallization during polymerization used in synthesizing the single crystals of PHBA was proven also for other polymers to be a means to produce extended-chain crystals which can be close to equilibrium [43]. Platelets of thicknesses in the chain direction of 0.3–3 μm were reported on crystallization during polymerization, having the same two orthorhombic structures [44]. In contrast, the thin lamellae had a length of only 100 Å, corresponding to oligomers of only about 15 repeating units [41].

The somewhat broader diffraction peaks in PHNA of Figs. 5 and 6 and its orthorhombic unit cell agrees well with the literature data ($a=7.66$ Å, $b=5.98$ Å, $c=17.12$ Å, $Pbc2_1$) [45]. To get a better fit of the calculated pattern, it was assumed that the chains are statistically disordered relative to their two possible directions, and experience a 1.7 Å shift along c. Geil and coworkers [46] resolved this difficulty by an analysis of electron diffraction patterns of PHNA from solution-polymerized whiskers (for the 100 and 010 reflections) and of thin-film, melt-polymerized lamellae (for the 001 reflection). Their results yielded a triclinic, pseudo-monoclinic unit cell ($a=7.712$ Å, $b=5.905$ Å, $c=17.202$ Å, $\alpha=\gamma=90°$, and $\beta=97.5°$) which also should fit the here presented results. Again, a wide variety of chemical as well as physical histories can produce differences in the diffraction patterns. The morphologies of well-crystallized samples ranged, as in PHBA, from fibrils [14], to thick lamellae [13], and thin lamellae [47,48].

The glass transitions for PHBA and PHNA are listed in Table 1 and are little different in temperature (434 and 420, respectively) and the increase in heat capacity is also rather small (33.9 and 45.2 J K^{-1} mol^{-1}, respectively). Such small changes are easily accounted for by the increase in deviation from strict linearity and size of the repeating unit [9]. Both values are based on the best estimate of T_g and an extrapolation of the heat capacity established in the melt and the solid state. At sufficiently low temperature, the heat capacity of the glass is close to that of the crystal. Due to the crystallinity, both glass transitions cover a wide range of temperature (57 and 214 K, respectively). For PHNA this means that the upper end of the glass transition reaches to the beginning of the lower disordering transition, which may account for the poorer crystallization of PHNA. An example for extreme hindrance of crystallization and melting by formation of a rigid-amorphous phase is poly(oxy-2,6-dimethyl-1,4-phenylene) [49]. In this case, the upper limit of the glass transition of the amorphous phase extends above the melting temperature.

The 95/5, 90/10, and 80/20 copolymers, as represented in Figs. 8–11 show a close relationship to the corresponding PHBA diffraction pattern, but decrease in peak intensity and increase in peak breadth, as one expects from decreasing crystallinity and crystal perfection. Relative to the more flexible polymers, such as poly(ethylene-*co*-propylene)s, this decrease in crystallinity is less. The latter lose all crystallinity when containing less than 20 branches per 100 chain atoms, despite of partial inclusion of the methyl branches in the polyethylene crystal. This limit of loss of all crystallinity decreases to 10 branches per 100 chain atoms for longer side groups which are fully excluded from the crystal [50]. A comparison of diffraction diagrams in Fig. 8 reveals that there is a continuity of changes in the crystal structures to the 90/10 copolymer, while the 80/20 diagram has already some character of the PHNA.

Unassigned patterns of commercial, drawn samples of copolymers with varying concentrations led to a similar conclusion that the diffraction pattern changes very gradually and between 50/50 and 40/60 HBA/HNA becomes more closely related to the PHNA pattern [51]. The absolute Bragg spacings of the fiber patterns, however, could not be compared to the data of Fig. 8. Diffraction patterns for a 75/25 HBA/HNA copolymer are available as a function of crystallization time at 505 K [18] and indicate a slow growing, orthorhombic structure with increasing lattice parameters of $a=8.16$ Å and $b=5.53$ Å (after 167 h), which compare to the 80/20 HBA/HNA unit cell of Fig. 11 which has a somewhat larger HNA concentration ($a=7.86$ Å, $b=5.60$ Å). In addition, a limited amount of fast growing hexagonal packing ($a=5.15$ Å) was observed in [18] which does not show in Fig. 11, but agrees with the 523 K pseudo-hexagonal diffraction. Similarly oriented sheets of a 73/27 HBA/HNA copolymer were analyzed as a function of annealing temperature [52] with similar results (orthorhombic $a=7.9$ Å, annealed at 543 K for 6 h, increasing at lower annealing temperatures; $b=5.5$ Å, annealed at 543 K for 6 h, decreasing at lower annealing temperatures; the pseudo-hexagonal is $a=5.16$ Å). The X-ray scattering diagram of a 66/34 HBA/HNA random copolymer (58/43 wt%) quenched and annealed for 100 h at 463 K was

reported, also observing a two-step crystallization, the annealed sample resembling Fig. 11 [6]. For higher molar masses the growth of the orthorhombic crystals took longer [53]. Confined thin film melt-polymerization yielded 100 Å thick single crystal lamellae of copolymers with 67/33, 50/50, and 33/67 HBA/HNA composition [54]. The electron diffraction suggests good lateral ordering of the molecules over large distances despite their random structure along the chain. Thicker films yielded superlattice structures with a high degree of order extending over tens of micrometers.

The glass transitions of the copolymers were only discovered after it was shown by quantitative thermal analysis that they covered such a broad temperature range that often no distinct change in the heat-flow rate could be observed [8,9]. The glass transition decreases only slightly in the mid-concentration range as shown in Table 1, and no hysteresis was reported. The broad vitrification range was confirmed by thermally stimulated current [55], and it was shown that in completely non-crystalline copolymer films the glass transition was more pronounced [56].

The copolymers, thus, follow more closely a solid-solution behavior with a gradual change from a structure being related to one homopolymer to the other. Under similar crystallization conditions, the crystallinity decreases with increasing co-monomer content, but it does not reach zero in the midrange of concentration. The remaining partial order is sufficient to broaden the glass transition over the whole concentration, seemingly without producing a distinct rigid-amorphous phase. Since the mobile phase at high temperature is liquid-crystal like, the non-crystalline portion of the partially ordered copolymers cannot not be fully amorphous either, as is common in most other semicrystalline polymers, but must remain anisotropic. Below the glass transition, in the solid state, the heat capacity is additive with concentration and corresponds to the crystalline heat capacity down to perhaps 50 K [9].

4.2. Condis crystals and disordering transitions

Raising the temperature of any of the homopolymers and copolymers beyond the glass transition leads to a disordering transition at T_1 as listed in Table 1. The change of a rigid crystal to an isotropic melt (fusion) is known to involve up to three different types of disordering, expressed as $\Delta S_f = \Delta S_{pos} + \Delta S_{orient} + \Delta S_{conf}$ [37], where S_f, S_{pos}, S_{orient} and S_{conf} denote the total, the positional, the orientational, and the conformational entropy of fusion, respectively. Empirical rules that describe these entropy changes have been developed: ΔS_{pos} is 7–14 J K^{-1} mol^{-1}, ΔS_{orient} ranges from 20 to 50 J K^{-1} mol^{-1}, and ΔS_{conf} is generally between 7 and 12 J K^{-1} mol^{-1} [15,57]. The values for ΔS_{pos} and ΔS_{orient} refer to the entire molecule, while ΔS_{conf} is per conformationally disordered flexible bond in the molecule. The polymeric nature of the samples precludes any major changes in ΔS_{pos} and ΔS_{orient} (which apply to the whole molecule), while the ΔS is too large for a crystal–crystal transition (which retains full three-dimensional order). The ΔS_{conf} is also not at its maximum level which for complete melting (full conformational disorder) should be, for rotation around two bonds in the range of 14–24 J K^{-1} mol^{-1} [poly(methylene) (1), 9.9; poly(propylene) (2), 18.9; poly (ethylene terephthalate) (5), 48.6; poly(trimethylene terephthalate) (6), 58.8 J K^{-1} mol^{-1}; (the number of bonds for possible rotations is in parentheses)] [37]. The magnitude of the transition entropies at T_1 for the single crystalline samples of PHBA (9.3 J K^{-1} mol^{-1}) and PHNA (10 J K^{-1} mol^{-1}) and the remaining three-dimensional order (gained from Figs. 3 and 6) indicate that this transition must be from a rigid crystal to a condis crystal, gaining about half of the possible disorder. In accord with the increased motion, the second phases are more symmetric in their X-ray structure than the orthorhombic, room-temperature phase.

For PHBA, the second transition entropy at 719 K is small (T_2, 0.5 J K^{-1} mol^{-1}), indicating a minor adjustment of the structure from pseudo-hexagonal to fully hexagonal. The polymer chains as a whole, however, retain their positional and translational order in all three crystallographic directions. This transition disappears after reaching more than 10 mol% HNA.

The transition from the condis crystals at T_3 has a large entropy change for PHNA (6.5 J K^{-1} mol^{-1}, see Table 1). The X-ray data show a transition to an anisotropic melt in form of a nematic liquid crystal, which implies loss of long-range positional order in two-dimensions. Chain correlation in the *c*-direction is retained, as evidenced by the presence of the 002 reflections in Fig. 6. A nematic liquid crystalline phase going to the melt disorders typically with less than 2.3 ± 1.5 J K^{-1} mol^{-1} (average of 279 transitions of small molecules, and only minor increases when going to macromolecules with flexible spacers) [57,37]. The total entropy of transition for all disorder gained from room temperature to the anisotropic melt via latent heats should thus be 20(+) J K^{-1} mol^{-1}, an entropy of fusion as expected for PHNA. For PHBA the T_3 transition was not observed by us because of excessive decomposition. The X-ray patterns in Fig. 2 are the only evidence, that the hexagonal phase exists up to at least 773 K and possibly higher. It is not clear if there is a transition into the anisotropic melt with a larger entropy of disordering before complete decomposition. The anisotropic melt phase is likely to exist, judged from the morphology of samples quenched from 753 K to room-temperature [12]. One would expect a somewhat smaller total entropy of transition for all disorder gained from room temperature to the anisotropic melt via latent heats than for PHNA since the rotation of the phenylene group about its two-fold axis could be a jump-like motion, and then not contribute to the entropy because of identical initial and final states before and after the jump.

Many thermal analyses have been presented in the past for the copolymers, but none, except those in [8,9] were made quantitative by evaluation of a heat capacity baseline. Approximate heats of transition, however, can also be extracted from calibrated heat-flow-rate curves, as shown in Fig. 1 by using empirical baselines. After calibrations and, if needed, lag corrections, the transition temperatures are also quite reproducible, but vary considerably with thermal and chemical history of the samples.

In summary, for both pure PHBA and PHNA, the first transition is to a condis crystal with a substantial ΔS_{conf}. This transition is accompanied by a 10–12% increase in unit cell volume, primarily in the cross-sectional area of the *a–b* plane. This is in concordance with the onset of conformational disorder of the phenylene and naphthalene units. Positional and translational long-range order, however, is retained in both cases; meaning that the polymer chains can be positioned on a three-dimensional crystal lattice. The second transition in PHBA is a minor transition from the pseudo-hexagonal to the hexagonal phase with a small latent heat and entropy. For PHNA the second transition is a major change from the condis crystal to an anisotropic melt, where long-range order is lost between chains in the *a–b* plane. For PHBA this transition could not be measured calorimetrically because of excessive decomposition.

4.3. Phase diagram

The present work can now be combined with prior work to provide a better understanding of the phase transitions for the entire copolymer system. The phase diagram is shown in Fig. 12 for the copolymers without annealing. Annealing results in additional transitions in the intermediate copolymer composition region. The hexagonal phase shown in the phase diagram is limited to the polymers with high-HBA content. The existence of a sharp second endotherm for PHNA was shown to involve a change of the condis crystal to a mobile, disordered mesophase with a significant entropy of transition. It leads to a change into a disordered mobile nematic mesophase, which may originate from the larger geometrical asymmetry of the HNA. The decomposition, as measured by thermogravimetry and X-ray diffraction, and the glass transition, from quantitative thermal analysis, limit the phase diagram to high and low temperatures, respectively. Overall the phase diagram refers to non-equilibrium since all throughout the sample is to be characterized as semicrystalline. Because of the overall presence of an anisotropic melt at the highest temperatures, the second phase should also be anisotropic instead of amorphous. A distinct, rigid-amorphous (or unisotropic) phase as a third phase does not seem to exist in this polymer system.

5. Conclusions

The low-temperature structure of all homopolymers and copolymers of the HBA/HNA system is orthorhombic and semicrystalline with a midrange of limited crystallinity. The second phase is represented by an anisotropic melt and below about 420 K, by an anisotropic glass. At higher temperatures the condis crystals of PHBA are pseudo-hexagonal and finally hexagonal. Molecules in these phases have conformational mobility and the disordering connected with this motion is confirmed by the entropies of transition and the existence of only few, diffuses X-ray reflections. The addition of the HNA to the PHBA provides a structural asymmetry and irregularity which retain a similar mesomorphic behavior to only about 10 mol%. A substantial crystallinity for the copolymers is the result of isomorphism of the HBA and HNA on a nanometer scale, modeled earlier by Biswas and Blackwell as a para-crystalline lattice structure, and by Windle and Coworkers as short-sequence matching into non-periodic layers. The PHNA as the second homopolymer can, again, attain higher degree of order than the copolymers and changes from an orthorhombic to a conformationally disordered phase. The resulting phase diagram in Fig. 12 combines the typical non-equilibrium data of Table 1 with the corresponding X-ray data as a guide to the overall system. The interpretation of the data was only possible by the combination of the structural data from X-ray diffraction with macroscopic, quantitative thermal analysis, linked to the microscopic molecular motion on identical samples. The general experiment-based description, using microscopic structure information and macroscopic thermodynamic data are linked to molecular motion, presents a picture that combines the many prior experiments published earlier. The phase diagram of Fig. 12, refers to a metastable system of a specific thermal and chemical history and must be adjusted for systems of different thermal, chemical, and mechanical pretreatment. The phase diagram is that of a solution in solid crystals and mobile mesophases.

Acknowledgements

This work was supported by the Division of Materials Research, National Science Foundation, Polymers Program, Grant # DMR-0312233, and by the Division of Materials Sciences and Engineering, Office of Basic Energy Sciences, US Department of Energy at Oak Ridge National Laboratory, managed and operated by UT-Battelle, LLC, for the US Department of Energy, under contract number DOE-AC05-00OR22725.

References

[1] Calundann GW, Jaffe M. Proc Robert A. Welch Found Conf Chem Res 1982;26:247.
[2] Ba GH, Cluff EF. In: Blumstein A, editor. Polymeric liquid crystals. New York: Plenum; 1985. p. 217.
[3] Dobb MG, McIntyre JE. Adv Polym Sci 1984;60/61:61.
[4] Stamatoff JB. Mol Cryst Liq Cryst 1984;110(1–4):75.
[5] Blackwell J, Biswas A. In: Ward IM, editor. Developments in oriented polymers-2. Barking, UK: Elsevier; 1987 [chapter 5].
[6] Butzbach GD, Wendorff JH, Zimmerman HJ. Makromol Chem Rapid Commun 1985;6:821.
[7] Butzbach GD, Wendorff JH, Zimmerman HJ. Polymer 1986;27:1337.
[8] Cao MY, Wunderlich B. J Polym Sci, Polym Phys Ed 1985;23:521.
[9] Cao MY, Varma-Nair M, Wunderlich B. Polym Adv Technol 1990;1:151.
[10] Cheng SZD. Macromolecules 1988;21:2475.
[11] Yoon DY, Masciocchi N, Depero LE, Viney C, Parrish W. Macromolecules 1990;23:1793.
[12] Economy J, Volksen W, Viney C, Geiss R, Siemens R, Karis T. Macromolecules 1988;21:2777.
[13] Mühlebach A, Lyerla J, Economy J. Macromolecules 1989;22:3741.
[14] Schwarz G, Kricheldorf HR. Macromolecules 1991;24:2829.

[15] Wunderlich B, Möller M, Grebowicz J, Baur H. Adv Polym Sci 1988; 87:1.
[16] Kricheldorf HR, Schwarz G. Polymer 1991;31:481.
[17] Ma J, Habenschuss A, Wunderlich B. Polymer. Submitted for publication.
[18] Cheng SZD, Janimak JJ, Zhang A, Zhou Z. Macromolecules 1989;22:4240.
[19] Biswas A, Blackwell J. Macromolecules 1988;21:3146.
[20] Biswas A, Blackwell J. Macromolecules 1988;21:3152.
[21] Biswas A, Blackwell J. Macromolecules 1988;21:3158.
[22] Hanna S, Lemmon T, Spontak RJ, Windle AH. Polymer 1992;33:3.
[23] Windle AH, Viney C, Golombok R, Donald AM, Mitchell GR. Trans Faraday Soc 1985;79:55.
[24] Hanna S, Windle AH. Polymer 1988;29:207.
[25] Wunderlich B. J Chem Phys 1958;29:1395.
[26] Langelaan HC, Posthuma de Boer A. Polymer 1996;37:5667.
[27] Kalika DS, Yoon DY. Macromolecules 1991;24:3404.
[28] Bechtholdt H, Wendorff JH, Zimmermann HJ. Macromol Chem 1987; 188:651.
[29] Calundann GW. US Patent 4,161,470; 1970.
[30] Kricheldorf HR, Schwarz G, Ruhser F. Macromolecules 1991;24:3485.
[31] Kricheldorf HR, Ruhser F, Schwarz G. Macromol Chem Phys 1991;192: 2371.
[32] Applemann DE. Indexing and least-square refinement of powder diffraction data, publ. PB-216 188, NITS, US Department of Commerce, 1973.
[33] Lieser G. J Polym Sci, Polym Phys Ed 1983;21:1611.
[34] Lieser G, Schwarz G, Kricheldorf HR. J Polym Sci, Polym Phys Ed 1983; 21:1599.
[35] Geiss R, Volksen W, Tsay J, Economy J. J Polym Sci, Polym Lett Ed 1984;22:433.
[36] Iannelli P, Yoon DY. J Polym Sci, Polym Phys Ed 1995;33:977.
[37] Wunderlich B. Thermal analysis of polymeric materials. Berlin: Springer; 2005.
[38] Liu J, Yuan B-L, Geil PH, Dorset DL. Polymer 1997;38:6031.
[39] Yuan B-L, Rybnikar F, Sasa P, Geil PH. J Polym Sci, Polym Phys Ed 1999;37:3532.
[40] Rybnikar F, Yuan B-L, Geil PH. Polymer 1994;35:1863.
[41] Rybnikar F, Liu J, Geil PH. Macromol Chem Phys 1994;195:81.
[42] Rybnikar F, Sasa P, Yuan B-L, Geil PH. J Polym Sci, Polym Phys Ed 1999;37:3520.
[43] Wunderlich B. Fortschr Hochpolymeren Forsch (Adv Polymer Sci) 1968; 5:568.
[44] Liu J, Geil PH. Polymer 1993;34:1366.
[45] Ianelly P, Yoon DY, Parrish W. Macromolecules 1994;27:3295.
[46] Liu J, Rybnikar F, Geil PH. Korea Polym J 1998;6:75.
[47] Rybnikar F, Liu J, Myers JA, Geil PH. Korea Polym J 1998;6:53.
[48] Liu J, Rybnikar F, Geil PH. J Macromol Sci-Phys 1993;B23:395.
[49] Pak J, Pyda M, Wunderlich B. Macromolecules 2003;36:495.
[50] Wunderlich B. Macromolecular physics. Crystal melting, vol. 3. New York: Academic Press; 1980.
[51] Gutierrez GA, Chivers RA, Blackwell J, Stamatoff JB, Yoon H. Polymer 1983;24:937.
[52] Kaito A, Kyotani M, Nakayama K. Macromolecules 1990;23:1035.
[53] Wilson DJ, Vonk CG, Windle AH. Polymer 1993;34:227.
[54] Liu J, Rybnikar F, Geil PH. J Macromol Sci-Phys 1996;B35:375.
[55] Sauer BB, Beckerbauer R, Wang L. J Polym Sci, Polym Phys Ed 1993;31: 1861.
[56] Yonetake K, Sagiya T, Koyama K, Masuko T. Macromolecules 1992;25: 1009.
[57] Wunderlich B, Grebowicz J. Adv Polym Sci 1984;60/61:1.